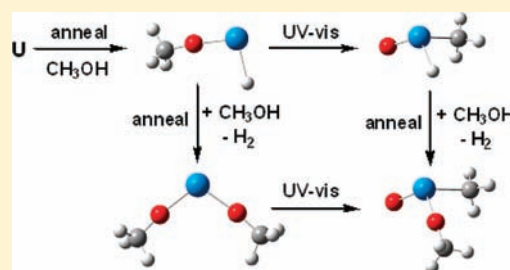


Matrix Infrared Spectroscopic and Theoretical Investigations of Uranium Atom and Methanol Reaction Products

Yu Gong and Lester Andrews*

Department of Chemistry, University of Virginia, Charlottesville, Virginia 22904-4319, United States

ABSTRACT: Reactions of laser-ablated uranium atoms and methanol are investigated in solid argon using matrix isolation and infrared spectroscopy. Four new product molecules are identified with the help of isotopically substituted methanol as well as density functional frequency calculations. Uranium atoms react spontaneously with methanol on annealing to form the U(II) insertion product CH_3OUH , which has a quintet ground state with strong C—O and U—H stretching vibrations. Further sample annealing allows the reaction of CH_3OUH and another methanol molecule to eliminate H_2 and give the $\text{U}(\text{OCH}_3)_2$ product. Near-UV–vis irradiation isomerizes the CH_3OUH molecule to the 32 kcal/mol lower energy U(IV) $\text{CH}_3\text{U}(\text{O})\text{H}$ isomer and the $\text{U}(\text{OCH}_3)_2$ molecule to the 28 kcal/mol lower energy $\text{CH}_3\text{OU}(\text{O})\text{CH}_3$ isomer. Both U(IV) products have triplet ground states, U=O double bonds, and pyramidal skeletal structures.



INTRODUCTION

The oxidation of methane to methanol is one of the most important subjects in the area of methane activation. Due to the relatively inert character of the C—H bond, effective catalysts are required to reduce the reaction barrier for the formation of the methanol product.¹ While a lot of effort has been spent on searching and optimizing catalysts with high activity and selectivity, studies on the reactions at molecular level also provide detailed insight into the mechanisms as well as the structures of intermediates in the methane oxidation process. Reactions of simple ionic and neutral metal oxide molecules and methane in both the gas phase and solid matrices are believed to be microscopic models for the methane oxidation process.^{2,3} As an alternative, useful information regarding the intermediates involved in the methane–methanol conversion can be derived from the reactions of metal atoms and methanol as well, which are the final products from methane and metal oxide reactions. A number of investigations on methanol reactions with main group and transition metal atoms have been carried out under cryogenic matrix conditions.^{4–11} Both O—H and C—O bond insertion product molecules have been characterized as major reaction products. Recent matrix isolation infrared spectroscopic investigations have revealed that early transition metal atoms can also react with two methanol molecules in solid argon to give the divalent $\text{M}(\text{OCH}_3)_2$ product with one H_2 molecule released.¹²

Although transition metal based catalysts are still widely used for methane oxidation, the catalytic properties of uranium have also been well recognized, which are far beyond its original applications in the nuclear industry.^{13,14} Previous studies in this laboratory have revealed that uranium atoms are capable of activating the C—H bonds of small hydrocarbons under suitable conditions.^{15–17} Hence it is interesting to probe the role of uranium in the methane–methanol conversion, which will be

helpful in understanding the methane oxidation process with uranium catalysts. In this paper, we report reactions of uranium atoms and CH_3OH in solid argon using matrix isolation infrared spectroscopy. Four new reaction intermediates are identified with the help of isotopic substitution as well as density functional theoretical calculations.

EXPERIMENTAL AND THEORETICAL METHODS

The experimental apparatus and procedure for investigating laser-ablated uranium atom reactions with CH_3OH during condensation in excess argon at 4 K have been described previously.¹⁸ The Nd:YAG laser fundamental (1064 nm, 10 Hz repetition rate with 10 ns pulse width) was focused onto a freshly cleaned uranium target (Oak Ridge National Laboratory, high purity, depleted of ^{235}U) mounted on a rotating rod. Laser-ablated uranium atoms were codeposited with 3–4 mmol of argon (Matheson, research) containing 0.5% CH_3OH onto a CsI cryogenic window for 60 min. Samples of CH_3OH (Omni Solv, 99.99%) or isotopic methanol, $^{13}\text{CH}_3\text{OH}$, $\text{CH}_3^{18}\text{OH}$, or CH_3OD (Cambridge Isotopic) samples were cooled to 77 K using liquid N_2 and evacuated to remove residual N_2 and O_2 before use. FTIR spectra were recorded at 0.5 cm^{-1} resolution on a Nicolet 750 FTIR instrument with a HgCdTe range B detector. Matrix samples were annealed at different temperatures and cooled back to 4 K for spectral acquisition. Selected samples were subjected to broadband photolysis with different filters by a medium-pressure mercury arc street lamp (Philips, 175W) with the outer globe removed.

Complementary density functional theory (DFT) calculations were performed using the Gaussian 09 program.¹⁹ The hybrid B3LYP density functional was employed in our calculations.²⁰ The 6-311++G(d,p) basis set was used for carbon, hydrogen, and oxygen atoms, and the 60

Received: March 25, 2011

Published: June 30, 2011

electron core SDD pseudopotential was used for uranium.^{21,22} The B3LYP functional combined with SDD basis set for uranium is adequate for describing the electronic structures of uranium containing molecules, which has been recently demonstrated in the experimental and theoretical studies on the reactions of uranium oxide anions and methanol in the gas phase.²³ All of the geometrical parameters were fully optimized, and the harmonic vibrational frequencies were obtained analytically at the optimized structures. In addition, geometry optimizations and frequency calculations using BPW91 pure density functional were also carried out on some product molecules for comparison.²⁴

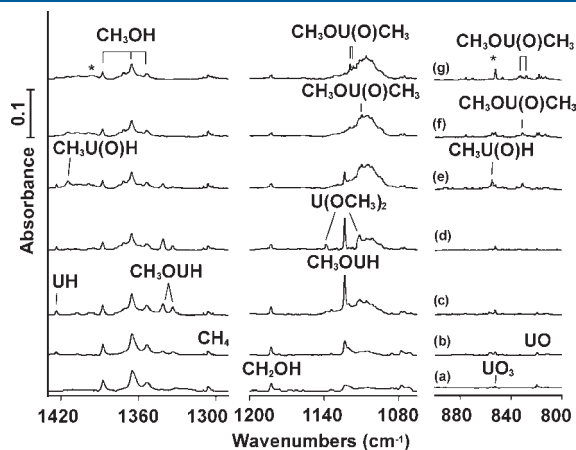


Figure 1. Infrared spectra of laser-ablated U atom and CH₃OH reaction products in solid argon: (a) U + 1.0% CH₃OH deposition for 60 min; (b) after annealing to 20 K; (c) after annealing to 30 K; (d) after annealing to 40 K; (e) after $\lambda > 290$ nm irradiation; (f) after $\lambda > 220$ nm irradiation; (g) after annealing to 35 K. The asterisks denote the (CH₃U(O)H)–(CH₃OH) complex absorptions.

RESULTS AND DISCUSSION

The infrared spectra from the reactions of laser-ablated uranium atoms and CH₃OH in solid argon are shown in Figure 1, and the product absorptions are listed in Table 1. After 1 h of sample deposition at 4 K, common absorptions due to the CH₂OH²⁵ and HCO²⁶ radicals, the solvated proton complex (Ar_nH⁺),²⁷ as well as the H₂CO and CH₄ molecules were observed. Weak uranium oxide absorptions were also present in the matrix sample after deposition.²⁸ All these absorptions decreased when the sample was annealed to successively higher temperatures while a series of absorptions previously assigned to methanol dimer²⁹ and the diatomic UH absorption³⁰ at 1423.6 cm⁻¹ appeared.

In addition to these known absorptions, new product bands at 1341.0 and 1123.3 cm⁻¹ increased markedly upon 20–30 K sample annealing, and weak 1137.9 and 1112.6 cm⁻¹ bands appeared (Figure 1, traces b and c). Next, annealing to 40 K decreased the former pair slightly and increased the latter pair 3-fold (trace d). Subsequent irradiation through a Pyrex ($\lambda > 290$ nm) filter reduced the 1341.0 and 1123.3 cm⁻¹ absorptions by 70% of their intensities and destroyed the 1137.9 and 1112.6 cm⁻¹ bands. At the same time, four new absorptions appeared at 1414.6, 854.7, 1109.6, and 830.8 cm⁻¹, and the weak methane absorption at 1305.6 cm⁻¹ increased slightly (Figure 1, trace e). Further broadband irradiation (trace f, $\lambda > 220$ nm) destroyed the 1341.0 and 1123.3 cm⁻¹ as well as the 1414.6 and 854.7 cm⁻¹ absorptions while the intensities of the 1109.6 and 830.8 cm⁻¹ absorptions were not changed. Subsequent sample annealing produced additional new absorptions at 1394.7, 852.1, 1118.9, 1116.5, 828.0, and 832.6 cm⁻¹, which were slightly shifted from the four absorptions that appeared after $\lambda > 290$ nm irradiation (Figure 1, trace g).

Table 1. Infrared Absorptions (cm⁻¹) Observed for the Products of the Reactions of Uranium Atoms and CH₃OH in Solid Argon^a

CH ₃ OH	¹³ CH ₃ OH	CH ₃ OH + ¹³ CH ₃ OH	CH ₃ ¹⁸ OH	CH ₃ OH + CH ₃ ¹⁸ OH	CH ₃ OD
CH ₃ OUH					
1341.0	1341.0	1341.0	1340.6	1340.8	956.7
(1333.5)	(1333.4)	(1333.5)	(1333.2)	(1333.5)	(952.1)
1123.3	1105.5	1123.3, 1105.5	1087.8	1123.3, 1087.8	1126.1
CH ₃ U(O)H					
1414.6	1414.6	1414.6	1414.6	1414.6	1002.1
[1394.7] ^b	[1394.6]	[1394.6]	[1394.6]	[1394.6]	[997.8]
854.7	854.6	854.7	809.6	854.8, 809.6	853.6
[852.1] ^b	[851.9]	[851.9]	[807.1]	[852.1, 807.1]	[851.0]
U(OCH ₃) ₂					
1137.9	1120.6	1138.3, 1132.1, 1120.6	1101.6	1137.5, 1129.0, 1101.6	1137.9
1112.6	1093.5	1112.3, 1099.2, 1093.5	1078.8	not obsd	1112.6
CH ₃ OU(O)CH ₃					
1109.6 ^c	1092.0	not obsd	1075.0	not obsd	not obsd
(1118.9) ^d	(1099.9)	(1118.8, 1099.9)	(1082.7)	(1118.9, 1082.8)	(1118.9)
(1116.5) ^d	(1096.3)	(1116.5, 1096.3)	(1080.4)	(1116.4, 1080.4)	(1116.4)
830.8 ^c	830.8	830.8	787.4	830.7, 787.4	not obsd
(828.0) ^d	(828.0)	(828.0)	(784.1)	(827.8, 783.8)	(828.0)
(832.6) ^d	(832.0)	(832.3)	(790.4)	(832.5, 790.4)	(832.7)

^a Frequencies in parentheses are matrix site absorptions. ^b The bracket values are probably due to a complex with CH₃OH, see text. ^c Bands produced on $\lambda > 290$ nm irradiation. ^d Matrix sites produced on annealing.

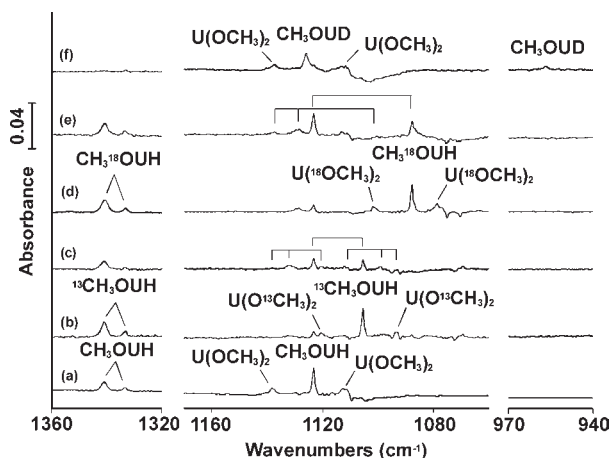


Figure 2. Infrared spectra of laser-ablated U atoms and isotopically substituted CH_3OH reaction products in solid argon (difference plotted: spectrum recorded after 40 K annealing minus spectrum recorded after $\lambda > 290$ nm irradiation): (a) U + 1.0% CH_3OH ; (b) U + 0.5% $^{13}\text{CH}_3\text{OH}$; (c) U + 0.5% CH_3OH + 0.5% $^{13}\text{CH}_3\text{OH}$; (d) U + 0.5% $\text{CH}_3^{18}\text{OH}$; (e) U + 0.5% CH_3OH + 0.5% $\text{CH}_3^{18}\text{OH}$; (f) U + 0.5% CH_3OD .

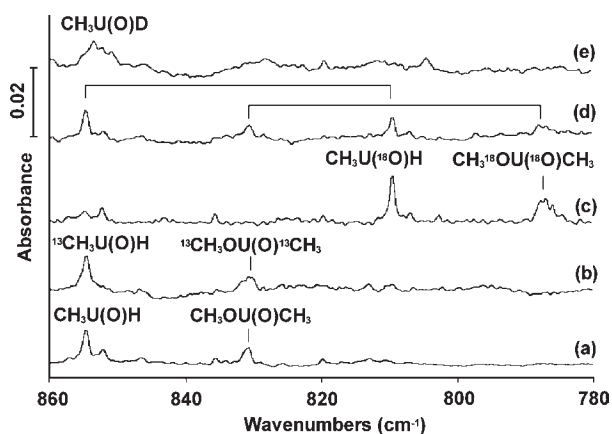


Figure 3. Infrared spectra of laser-ablated U atoms and isotopically substituted CH_3OH reaction products in solid argon at 4 K after $\lambda > 290$ nm irradiation: (a) U + 1.0% CH_3OH ; (b) U + 0.5% $^{13}\text{CH}_3\text{OH}$; (c) U + 0.5% $\text{CH}_3^{18}\text{OH}$; (d) U + 0.5% CH_3OH + 0.5% $\text{CH}_3^{18}\text{OH}$; (e) U + 0.5% CH_3OD .

All of the experiments were repeated using $^{13}\text{CH}_3\text{OH}$, mixed $\text{CH}_3\text{OH} + ^{13}\text{CH}_3\text{OH}$, $\text{CH}_3^{18}\text{OH}$, and mixed $\text{CH}_3\text{OH} + \text{CH}_3^{18}\text{OH}$ samples to help identify the products. All products gave isotopic doublets containing the same absorptions as in the pure isotopic experiments using the mixed isotopic samples except for the 1137.9 and 1126.6 cm^{-1} bands which produced triplets. The additional band in the triplet provides evidence for a product that requires two methanol molecules. An experiment with CH_3OD sample was also done to characterize possible U–H stretching modes in the new products. Infrared spectra from the reactions of uranium atoms with isotopically substituted samples are shown in Figures 2 and 3 and the experimental vibrational frequencies listed in Table 1.

CH_3OUH . The 1341.0 and 1123.3 cm^{-1} absorptions increased together on 20–30 K annealing and decreased in concert on UV

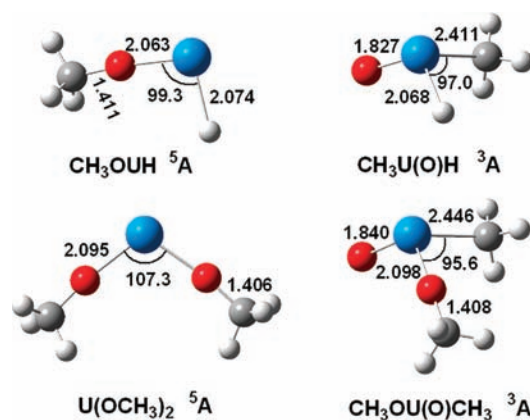


Figure 4. Structures of the products from the reactions of uranium atoms and methanol calculated at the DFT/B3LYP level of theory (bond lengths in angstrom units and bond angles in degrees).

irradiation so they are probably due to different vibrational modes of the same molecule on the basis of their common behavior. The 1123.3 cm^{-1} absorption shifted to 1105.5 and 1087.8 cm^{-1} , respectively, in the experiments with $^{13}\text{CH}_3\text{OH}$ and $\text{CH}_3^{18}\text{OH}$ samples. The $^{12}\text{C}/^{13}\text{C}$ and $^{16}\text{O}/^{18}\text{O}$ frequency ratios are 1.0161 and 1.0326, which are higher than the corresponding 1.0152 and 1.0254 ratios for methanol, but they bracket the characteristic ratios, 1.0225 and 1.0245, for the diatomic molecule C–O stretching vibration. The higher $^{16}\text{O}/^{18}\text{O}$ frequency ratio for CH_3OUH suggests that this mode has antisymmetric C–O–metal stretching character. No intermediate absorption was observed in the mixed isotopic experiments (Figure 2, traces c and e), indicating the involvement of only one C–O moiety in this mode. For the upper band at 1341.0 cm^{-1} , reaction with $^{13}\text{CH}_3\text{OH}$ sample had no effect, and only a small red shift of 0.4 cm^{-1} was observed with $\text{CH}_3^{18}\text{OH}$ sample. However, a large 384.3 cm^{-1} shift to 956.7 cm^{-1} was found in the CH_3OD experiment with H/D frequency ratio 1.4017 (Figure 2, trace f), which is almost the same as that of diatomic UH molecule (H/D ratio 1.4008).³⁰ Hence the 1341.0 cm^{-1} absorption is assigned to the U–H stretching vibration of the new molecule, which results from U insertion into the O–H bond of methanol. Note that the 1123.3 cm^{-1} band shifts higher to 1126.1 cm^{-1} in the deuterated species, which requires interaction with a lower (U–D) mode as described above. On the basis of the two experimentally observed infrared absorptions, CH_3OUH is proposed as the product molecule.

Identification of the CH_3OUH molecule is supported by density functional calculations. Figure 4 shows the optimized geometry of the CH_3OUH molecule in its quintet ground state. The U–H bond length of this insertion product is calculated to be 2.074 Å, similar to that in known UH containing species.^{30–32} The C–O bond length is predicted to be 1.411 Å, in the region of typical C–O single bonds.^{8,9} Frequency calculations at the B3LYP level predict that the CH_3OUH molecule has its two strongest infrared absorptions at 1321.6 and 1126.1 cm^{-1} (Table 2). Although the computed 1321.6 cm^{-1} frequency is slightly lower than the absorption observed at 1341.0 cm^{-1} , the experimental and theoretical H/D ratios are almost the same (Table 3), which characterizes a U–H stretching vibrational mode. The calculation also predicts the blue deuterium shift for the C–O stretch owing to different interactions with the higher U–H and lower U–D stretching modes. This C–O stretching

Table 2. Total Energies (in Atomic Units, after Zero Point Energy Correction), Frequencies (cm^{-1}), and Intensities (km/mol) of the Observed Products Calculated at the B3LYP Level^a

	energy	frequencies (intensities)
CH_3OUH (^5A)	-592.666285	3067.1 (33), 3063.0 (37), 3000.0 (121), 1494.2 (6), 1493.6 (3), 1470.5 (7), 1321.6 (473), 1166.2 (2), 1165.6 (2), 1126.1 (460), 437.5 (69)
$\text{CH}_3\text{U(O)H}$ (^3A)	-592.716509	3049.8 (18), 3033.2 (27), 2964.2 (15), 1432.4 (8), 1418.5 (15), 1372.8 (463), 1162.2 (7), 861.0 (259), 470.4 (11), 443.4 (133)
$\text{U(OCH}_3)_2$ (^5A)	-707.285703	3044.7 (81), 3044.5 (2), 3043.0 (40), 3042.4 (49), 2986.1 (125), 2984.0 (161), 1495.4 (0), 1494.9 (7), 1494.4 (5), 1494.0 (2), 1471.3 (8), 1469.4 (12), 1169.6 (1), 1167.0 (4), 1166.9 (2), 1166.3 (0), 1142.1 (308), 1114.7 (515), 421.7 (16), 407.8 (91)
$\text{CH}_3\text{OU(O)CH}_3$ (^3A)	-707.331107	3057.1 (28), 3054.7 (40), 3051.4 (41), 3030.7 (35), 2991.1 (118), 2966.2 (30), 1494.7 (4), 1492.8 (5), 1470.9 (10), 1438.9 (2), 1427.5 (5), 1167.3 (5), 1165.9 (2), 1152.3 (4), 1122.8 (412), 836.4 (274), 478.4 (25), 448.1 (30), 412.2 (46)

^a Only the absorptions above 400 cm^{-1} are listed.

Table 3. Comparison Between the Observed and Calculated (B3LYP) Vibrational Frequencies (cm^{-1}) and Isotopic Frequency Ratios of the Products

mode	frequencies		$^{12}\text{C}/^{13}\text{C}$		$^{16}\text{O}/^{18}\text{O}$		H/D ^a	
	calcd	obsd	calcd	obsd	calcd	obsd	calcd	obsd
CH_3OUH (^5A)								
U—H str	1321.6	1341.0	1.0001	1.0000	1.0005	1.0003	1.4156	1.4017
C—O—U str	1126.1	1123.3	1.0160	1.0161	1.0337	1.0326	0.9960	0.9975
$\text{CH}_3\text{U(O)H}$ (^3A)								
U—H str	1372.8	1414.6	1.0001	1.0000	1.0002	1.0000	1.4038	1.4116
U=O str	861.0	854.7	1.0001	1.0000	1.0562	1.0557	1.0043	1.0013
$\text{U(OCH}_3)_2$ (^5A)								
sym C—O—U str	1142.1	1137.9	1.0158	1.0154	1.0342	1.0330	1.0000	1.0000
antisym C—O—U str	1114.7	1112.6	1.0173	1.0175	1.0323	1.0313	1.0000	1.0000
$\text{CH}_3\text{OU(O)CH}_3$ (^3A)								
C—O—U str	1122.8	1109.6	1.0164	1.0161	1.0334	1.0322	1.0000	not obsd
U=O str	836.4	830.8	1.0002	1.0000	1.0563	1.0551	1.0000	not obsd

^a D refers to CH_3OD reaction product.

mode calculated at 1126.1 cm^{-1} is 2.8 cm^{-1} higher than the experimental frequency with $^{12}\text{C}/^{13}\text{C}$ and $^{16}\text{O}/^{18}\text{O}$ frequency ratios almost identical with those observed in the experiment. In order to compare with the hybrid B3LYP functional, the BPW91 pure density functional was also used to probe the structural parameters and vibrational frequencies of the CH_3OUH molecule. The above stretching modes were computed as 1316.0 cm^{-1} (433 km/mol) and 1093.5 cm^{-1} (385 km/mol) with U—O, U—H, and C—O bond lengths of 2.048, 2.055, and 1.417 Å. The usual trend of B3LYP frequencies slightly higher than BPW91 values holds here.³³

$\text{CH}_3\text{U(O)H}$. The 1414.6 and 854.7 cm^{-1} absorptions were produced on irradiation at the expense of the insertion product, suggesting that this new product is probably a structural isomer of the CH_3OUH molecule. No shift was found for the absorption at 1414.6 cm^{-1} using all of the isotopic substituted precursors except for CH_3OD , where the deuterium counterpart was observed at 1002.1 cm^{-1} . The large H/D frequency ratio (1.4116) observed for the 1414.6 cm^{-1} absorption indicates

assignment to a U—H stretching mode, which falls between the two U—H stretching frequencies for H_2UO at 1416.3 and 1377.1 cm^{-1} .³¹ Small 0.1 and 1.1 cm^{-1} isotopic shifts were found for the 854.7 cm^{-1} absorption with $^{13}\text{CH}_3\text{OH}$ and CH_3OD samples, respectively, but the corresponding absorption in the $\text{CH}_3^{18}\text{OH}$ experiment was observed at 809.6 cm^{-1} (Figure 3). This 45.1 cm^{-1} red shift from the frequency with CH_3OH defines the $^{16}\text{O}/^{18}\text{O}$ ratio (1.0557), which is about the same as for the diatomic UO molecule (1.0571)²⁸ and is characteristic of a U=O stretching vibration. The observation of these two diagnostic vibrational modes supports assignment of the 1414.6 and 854.7 cm^{-1} absorptions to the U—H and U=O stretching modes of the $\text{CH}_3\text{U(O)H}$ molecule. As found in other molecules with U—C single bonds,^{15–17} the unobserved U—C stretching band falls at the spectral limit, where this band cannot be observed due to poor signal-to-noise.

To verify our identification of the new product, density functional calculations were carried out. Geometry optimization of the $\text{CH}_3\text{U(O)H}$ molecule converged to a nonplanar structure

with triplet ground state (Figure 4). The U=O bond length is calculated to be 1.827 Å, which is about the same as the U=O double bond calculated for the UO and H₂UO molecules.^{28,31} A strong U=O vibration is predicted at 861.0 cm⁻¹ for the CH₃U(O)H molecule, 6.3 cm⁻¹ higher than the experimentally observed 854.7 cm⁻¹ frequency. The ¹⁶O/¹⁸O frequency ratio is also consistent with the value from our calculations (Table 3). Similar to the insertion product, our B3LYP calculation underestimated the experimental U—H stretching frequency of the CH₃U(O)H molecule by 41.8 cm⁻¹. However, the theoretical H/D frequency ratio is almost identical to the experimental value, which supports our assignment. The U—H bond length is found to be 2.068 Å, which falls into the region for typical U—H bonds.³⁰ In addition, the pure density functional BPW91 was used for calculation. The above stretching modes were computed as 1414.4 cm⁻¹ (429 km/mol) and 846.0 cm⁻¹ (208 km/mol) with U=O, U—H, and U—C bond lengths of 1.827, 2.039, and 2.379 Å. The usual trend of B3LYP frequencies slightly higher than BPW91 values³³ holds for the U=O bond, with the observed value between the two functional calculated values, but the BPW91 calculation for the U—H stretching mode finds a 42 cm⁻¹ higher value fortuitously in agreement with the observed value. These comparisons underscore the approximate nature of DFT frequency calculations, and BPW91 finds a slightly stronger U—H bond than B3LYP.

The CH₃U(O)H molecule has a similar pyramidal structure with the CH₃M(O)H (M = Ti, Nb, Ta) molecules reported previously.^{34,35} Bonding analysis reveals that the two unpaired electrons in CH₃U(O)H are mainly localized in two f orbitals. A similar geometry was also found for the H₂UO molecule from the reactions of uranium atoms and water.³¹ Our calculations at the B3LYP level of theory revealed that the U=O bond length of the H₂UO molecule is slightly shorter by 0.004 Å, nearly the same as for the CH₃U(O)H molecule. Consistent with this trend, the U=O stretching frequency for the CH₃U(O)H molecule is only about 5 cm⁻¹ lower than that of H₂UO.

The 1394.7 and 852.1 cm⁻¹ absorptions, which appeared on final annealing, are attributed above to environmental effects on the nearby 1414.6 and 854.7 cm⁻¹ bands. The breadth and 20 cm⁻¹ shift of the U—H stretching mode suggests a (CH₃U(O)H)—(CH₃OH) complex with interaction through the U—H bond.

U(OCH₃)₂. Two absorptions at 1137.9 and 1112.6 cm⁻¹ were produced upon annealing to 30–40 K, and during the last annealing the intensity of the CH₃OUH absorptions decreased slightly. Hence the formation of this new species probably involves the reaction of CH₃OUH and another methanol molecule as methanol dimer absorptions also increase on annealing. Frequency shifts with ¹³CH₃OH and CH₃¹⁸OH samples revealed that the 1137.9 and 1112.6 cm⁻¹ absorptions are due to C—O—U stretching modes. In the mixed CH₃OH + ¹³CH₃OH experiment, two triplets were observed with the intermediate absorptions at 1132.1 and 1099.2 cm⁻¹ (Figure 2), suggesting the existence of two equivalent C—O moieties in this new molecule. Since no other absorption was found to have identical behaviors with the 1137.9 and 1112.6 cm⁻¹ absorptions, we assign these two bands to the symmetric and antisymmetric C—O—U stretching vibrations of the U(OCH₃)₂ molecule.

Our B3LYP calculations predict this molecule to have a quintet ground state with C₂ symmetry. As listed in Table 2, the infrared absorptions predicted at 1142.1 and 1114.7 cm⁻¹ for symmetric and antisymmetric C—O—U stretches are much stronger than the others. The observed 1137.9 and 1112.6 cm⁻¹ frequencies

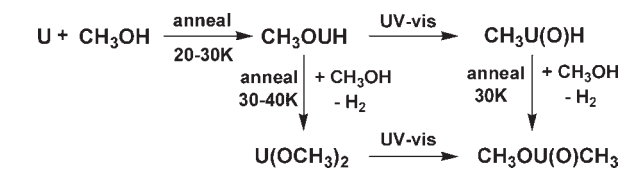
correlate nicely with the above predictions. Further support for our assignment of the U(OCH₃)₂ molecule can be found from the good correlation between experimental and theoretical isotopic ratios (Table 3). Similar to the U(OH)₂ molecule identified in the reactions of uranium and H₂O₂,³⁶ the U(OCH₃)₂ molecule also has a bent geometry with the OUO bond angle of 107.3°. As a result, the antisymmetric C—O—U stretching mode is less than twice as strong as the symmetric one, which is different from the titanium and vanadium analogues with linear structures.¹²

CH₃OU(O)CH₃. The 1109.6 and 830.8 cm⁻¹ absorptions increased together with λ > 290 nm irradiation. Isotopic substitution revealed ¹²C/¹³C and ¹⁶O/¹⁸O frequency ratios for the 1109.6 cm⁻¹ absorption of 1.0161 and 1.0322, respectively, similar to the above values for the C—O—U vibration in CH₃OUH. Following the 854.7 cm⁻¹ absorption of the CH₃U(O)H molecule, the 830.8 cm⁻¹ absorption also appeared in the U=O stretching region. This band was not shifted in the experiments with ¹³CH₃OH, but it shifted to 787.4 cm⁻¹ when uranium atoms reacted with CH₃¹⁸OH. Both the band position and the ¹⁶O/¹⁸O frequency ratio (1.0551) indicate that the 830.8 cm⁻¹ absorption is due to a U=O stretching mode. Only one U=O subunit is involved in this mode, which is evidenced by the doublet from the experiment with mixed CH₃OH + CH₃¹⁸OH sample (Figure 3). On the basis of observation of the 1109.6 and 830.8 cm⁻¹ absorptions, the new molecule should have a CH₃OU(O) moiety, and this formation requires two methanol molecules. However, no U—H stretching absorption was found to track with these two bands, nor did we observe the formation of methyl radical at 617 cm⁻¹.³⁷ As a result, the CH₃OU(O)CH₃ structure with one methoxyl group and one methyl group attached to the uranium center of UO is proposed for the candidate molecule, which absorbs at 1109.6 and 830.8 cm⁻¹. The 1118.9, 1116.5, 828.0, and 832.6 cm⁻¹ absorptions exhibited similar isotopic shifts with the absorptions at 1109.6 and 830.8 cm⁻¹, suggesting that these four bands are also due to the CH₃OU(O)CH₃ molecule but related by environmental matrix shifts.

The CH₃OU(O)CH₃ molecule is predicted by B3LYP calculations to have a triplet ground state with a pyramidal geometry. The two strongest infrared absorptions due to U=O and C—O—U stretching modes are calculated at 836.4 and 1122.8 cm⁻¹ (Table 2), which are 5.6 and 13.2 cm⁻¹ higher than the experimental frequencies. The ¹²C/¹³C and ¹⁶O/¹⁸O frequency ratios predicted from isotopic calculations are also in good agreement with the experimental values (Table 3). Geometry optimization for the CH₃OU(O)CH₃ molecule results in a U=O bond length of 1.840 Å, which is 0.013 Å longer than that in the newly identified CH₃U(O)H molecule (Figure 4). Experimentally, the U=O stretching frequency of the CH₃OU(O)CH₃ molecule is about 25 cm⁻¹ lower than that of the CH₃U(O)H molecule. Mulliken charge calculations reveal that more electron density is transferred from the uranium center to the methoxyl group in the CH₃OU(O)CH₃ molecule (CH₃O, -0.52 e; U, 1.58 e) than to the hydrogen atom in the CH₃U(O)H molecule (H, -0.32 e; U, 1.27 e) due to the strong electronegative character of the CH₃O group. As a result, a slightly weaker U=O bond is formed when the hydrogen atom in the CH₃U(O)H molecule is replaced by the methoxyl group owing to lower electron density in the uranium—oxygen π bond.

Reactions in the Matrix. The reactions of uranium atoms and methanol molecules in solid argon can be summarized as follows on the basis of the experimental observations.

Scheme 1



The infrared spectra in Figure 1 show that the CH_3OUH molecule was produced spontaneously when the sample was annealed to 20–30 K, suggesting that no activation energy is required for U insertion into the OH bond. Similar insertion reactions were also observed in previous experiments involving the reactions of scandium atoms and methanol, where insertion into the O–H bond is favored due to the low energy barrier.⁹ Formation of the CH_3OUH molecule upon sample annealing also shows that a $\text{U}(\text{CH}_3\text{OH})$ complex is not stabilized in the matrix. In our experiments, no absorption can be assigned to such a molecular complex, which is predicted by B3LYP calculation to have strong absorptions at 967 and 1320 cm^{-1} . The experimental absence of this complex is probably due to a low insertion reaction barrier to form the CH_3OUH molecule. In addition to the O–H insertion product, our calculations also predict another stable insertion isomer, CH_3UOH , which has a strong absorption at 592 cm^{-1} due to the U–OH stretch. Although the latter molecule is found to be 20 kcal/mol lower in energy than the experimentally identified CH_3OUH isomer, no new infrared absorption is observed in the region below 600 cm^{-1} . Although the formation of the CH_3UOH molecule is a thermodynamically favored process, we suggest that it is easier for U to insert into the O–H rather than the C–O bond, as observed in the reactions of scandium and methanol,⁹ although C–O insertion has been observed for Be and Mg reactions.^{7,8} Along this line, it is interesting to note that only hydrogen and CH_3O species were observed from methanol adsorbed on a polycrystalline uranium surface at low temperature while C–O bond dissociation did not occur until 200 K was reached.³⁸ This phenomenon implies that O–H bond dissociation is kinetically favored, but activation energy is required for the dissociation of the C–O bond on a uranium metal surface.

The initially formed uranium(II) molecule CH_3OUH can undergo isomerization under UV–vis irradiation to form the uranium(IV) molecule $\text{CH}_3\text{U}(\text{O})\text{H}$, which is more stable by 32 kcal/mol (B3LYP) or 40 kcal/mol (BPW91) and also the most stable product from the bimolecular reaction of uranium and methanol computed here (Table 2). This process is probably hindered by an energy barrier since the formation of the $\text{CH}_3\text{U}(\text{O})\text{H}$ product requires rearrangement of the methyl group from oxygen to the uranium center. Recent studies on the reactions of group IV and V transition metal oxides and methane have characterized a series of $\text{CH}_3\text{M}(\text{O})\text{H}$ molecules where the metal centers are in high oxidation states.^{34,35} Uranium is known to have several oxidation states,³⁹ which makes it possible for uranium to form the very stable uranium(IV) $\text{CH}_3\text{U}(\text{O})\text{H}$ molecule under suitable conditions. However, the uranium(VI) singlet state $\text{H}_2\text{C}=\text{U}(\text{O})\text{H}_2$ methyldiene bis-dihydride is 43 kcal/mol higher in energy and not observed here.

Annealing to 30–40 K allows the diffusion and association of methanol molecules²⁹ and the spontaneous reaction of CH_3OUH with another methanol molecule to form the $\text{U}(\text{OCH}_3)_2$ molecule with hydrogen elimination (Scheme 1), which is exothermic by

47 kcal/mol (B3LYP). It has been recently demonstrated that early transition metal atoms react spontaneously with two methanol molecules to release H_2 and to form the $\text{M}(\text{OCH}_3)_2$ products.¹²

Irradiation with UV–vis photons also produced the $\text{CH}_3\text{OU}(\text{O})\text{CH}_3$ molecule, similar to the above rearrangement, and this uranium(IV) molecule is 28 kcal/mol lower energy than the uranium(II) molecule $\text{U}(\text{OCH}_3)_2$. It also appears that $\text{CH}_3\text{U}(\text{O})\text{H}$ can add another methanol and eliminate hydrogen to form $\text{CH}_3\text{OU}(\text{O})\text{CH}_3$ on annealing with 44 kcal/mol (B3LYP) energy released, which probably accounts for the appearance of the related matrix site absorptions at 1118.9, 1116.5, 828.0, and 832.6 cm^{-1} . Finally, the uranium(VI) molecule $(\text{CH}_3)_2\text{UO}_2$, which is analogous to H_2UO_2 observed in the reaction with water,³¹ is calculated to be 10 kcal/mol more stable than the uranium(IV) molecule $\text{CH}_3\text{OU}(\text{O})\text{CH}_3$. However, based on no observation of its strong diagnostic antisymmetric O–U–O stretching mode computed at 950 cm^{-1} , this U(VI) molecule is not observed here.

Decomposition of the CH_3OUH and $\text{CH}_3\text{U}(\text{O})\text{H}$ molecules to methane and UO was also observed with ultraviolet irradiation (Figure 1, trace f, slight increase in CH_4 absorption at 1305.6 cm^{-1}). In contrast, no decomposition of methanol was observed under the same condition without the participation of uranium atoms, showing that involvement of uranium significantly reduces the reaction barrier for the CH_3OH to CH_4 conversion most likely through the abstraction of oxygen to form the very stable uranium monoxide. Some of the diatomic UO molecules produced upon UV irradiation are slightly perturbed by other molecules in the matrix, which is evidenced by the weak absorptions on the lower side of the isolated UO band. The weakly bound $\text{UO}(\text{CH}_4)$ complex probably absorbs in this region.

Gas phase studies using mass spectrometry revealed that the $\text{U}(\text{OH})_{1,2}^+$ and $\text{U}(\text{OR})_{1,2}^+$ cations were the major products from reactions of alcohol molecules and U^+ cations.⁴⁰ These molecular cationic species were proposed to be produced via C–O and O–H bond cleavage by uranium cations. However, only reactions with negligible activation energy can occur in the solid matrix during sample annealing, and the initially formed energetic intermediate molecules can be relaxed and stabilized by the surrounding matrix atoms. As a result, the CH_3OUH molecule is observed as the direct reaction product of uranium and methanol in solid argon. The CH_3UOH molecule as well as other dehydrogenation products cannot be produced spontaneously in the cryogenic matrix most likely for kinetic reasons.

As observed in the U and CH_3OH codeposition, absorptions due to CH_2OH , HCO and H_2CO were present in the matrix right after sample preparation, which is common in experiments with laser-ablated metal atoms and methanol.^{7–9} The formation of these three species indicates that some methanol molecules photodissociate during sample deposition due to irradiation from the plume produced by laser ablation.^{18,41} Both hydrogen atoms and molecules are produced along with the formation of the CH_2OH , HCO, and H_2CO molecules, which account for the growth of uranium hydride absorptions on sample annealing.

CONCLUSIONS

Diagnostic infrared absorptions for the CH_3OUH , $\text{CH}_3\text{U}(\text{O})\text{H}$, $\text{U}(\text{OCH}_3)_2$, and $\text{CH}_3\text{OU}(\text{O})\text{CH}_3$ molecules are obtained in solid argon at 4 K. The product molecules are prepared by reactions of laser-ablated uranium atoms with methanol

and characterized using matrix isolation infrared spectroscopy. The identifications of these molecules are supported by experiments with $^{13}\text{CH}_3\text{OH}$, $\text{CH}_3^{18}\text{OH}$, and CH_3OD samples as well as density functional frequency and energy calculations. These experiments show that ground state uranium atoms react with methanol to form the U(II) CH_3OUH molecule during sample annealing, which can add another methanol molecule to give $\text{U}(\text{OCH}_3)_2$. These rearrange to the U(IV) isomers $\text{CH}_3\text{U}(\text{O})\text{H}$ and $\text{CH}_3\text{OU}(\text{O})\text{CH}_3$ under $\lambda > 290$ nm irradiation. Both the $\text{CH}_3\text{U}(\text{O})\text{H}$ and $\text{CH}_3\text{OU}(\text{O})\text{CH}_3$ molecules are predicted to have triplet ground states with pyramidal structures. The $\text{U}=\text{O}$ double bond in the $\text{CH}_3\text{OU}(\text{O})\text{CH}_3$ molecule is slightly weaker than that in the $\text{CH}_3\text{U}(\text{O})\text{H}$ molecule due to the replacement of hydrogen by the methoxyl group.

AUTHOR INFORMATION

Corresponding Author

*E-mail: lsa@virginia.edu.

ACKNOWLEDGMENT

We gratefully acknowledge financial support from DOE Grant DE-SC0001034 and NCSA computing Grant CHE07-0004N.

REFERENCES

- (1) Crabtree, R. H. *Chem. Rev.* **2010**, *110*, 575.
- (2) (a) Roithová, J.; Schröder, D. *Chem. Rev.* **2010**, *110*, 1070. (b) Schröder, D.; Schwarz, H. *Proc. Natl. Acad. Sci. U.S.A.* **2008**, *105*, 18114.
- (3) Wang, G. J.; Zhou, M. F. *Int. Rev. Phys. Chem.* **2008**, *27*, 1.
- (4) Park, M.; Hauge, R. H.; Kafafi, Z. H.; Margrave, J. L. *J. Chem. Soc., Chem. Commun.* **1985**, 1570.
- (5) Maier, G.; Reisenauer, H. P.; Egenolf, H. *Monatsh. Chem.* **1999**, *130*, 227.
- (6) Khabashesku, V. N.; Kudin, K. N.; Margrave, J. L.; Fredin, L. *J. Organomet. Chem.* **2000**, *595*, 248.
- (7) Huang, Z. G.; Chen, M. H.; Liu, Q. N.; Zhou, M. F. *J. Phys. Chem. A* **2003**, *107*, 11380.
- (8) Huang, Z. G.; Chen, M. H.; Zhou, M. F. *J. Phys. Chem. A* **2004**, *108*, 3390.
- (9) Chen, M. H.; Huang, Z. G.; Zhou, M. F. *J. Phys. Chem. A* **2004**, *108*, 5950.
- (10) Joly, H. A.; Howard, J. A.; Artega, G. A. *Phys. Chem. Chem. Phys.* **2001**, *3*, 750.
- (11) Lanzisera, D. V.; Andrews, L. *J. Phys. Chem. A* **1997**, *101*, 1482.
- (12) Wang, G. J.; Su, J.; Gong, Y.; Zhou, M. F.; Li, J. *Angew. Chem., Int. Ed.* **2010**, *49*, 1302.
- (13) Fox, A. R.; Bart, S. C.; Meyer, K.; Cummins, C. C. *Nature* **2008**, *455*, 341.
- (14) Andrea, T.; Eisen, M. S. *Chem. Soc. Rev.* **2008**, *37*, 550.
- (15) (a) Lyon, J. T.; Andrews, L.; Malmqvist, P. Å; Roos, B. O.; Yang, T.; Bursten, B. E. *Inorg. Chem.* **2007**, *46*, 4917. (b) Cho, H.-G.; Lyon, J. T.; Andrews, L. *J. Phys. Chem. A* **2008**, *112*, 6902.
- (16) Cho, H.-G.; Andrews, L. *J. Phys. Chem. A* **2009**, *113*, 5073.
- (17) Andrews, L.; Kushto, G. P.; Marsden, C. J. *Chem.—Eur. J.* **2006**, *12*, 8324.
- (18) (a) Andrews, L.; Citra, A. *Chem. Rev.* **2002**, *102*, 885. (b) Andrews, L. *Chem. Soc. Rev.* **2004**, *33*, 123.
- (19) Frisch, M. J.; Trucks, G. W.; Schlegel, H. B.; Scuseria, G. E.; Robb, M. A.; Cheeseman, J. R.; Scalmani, G.; Barone, V.; Mennucci, B.; Petersson, G. A.; Nakatsuji, H.; Caricato, M.; Li, X.; Hratchian, H. P.; Izmaylov, A. F.; Bloino, J.; Zheng, G.; Sonnenberg, J. L.; Hada, M.; Ehara, M.; Toyota, K.; Fukuda, R.; Hasegawa, J.; Ishida, M.; Nakajima, T.; Honda, Y.; Kitao, O.; Nakai, H.; Vreven, T.; Montgomery, J. A., Jr.; Peralta, J. E.; Ogliaro, F.; Bearpark, M.; Heyd, J. J.; Brothers, E.; Kudin, K. N.; Staroverov, V. N.; Kobayashi, R.; Normand, J.; Raghavachari, K.; Rendell, A.; Burant, J. C.; Iyengar, S. S.; Tomasi, J.; Cossi, M.; Rega, N.; Millam, N. J.; Klene, M.; Knox, J. E.; Cross, J. B.; Bakken, V.; Adamo, C.; Jaramillo, J.; Gomperts, R.; Stratmann, R. E.; Yazyev, O.; Austin, A. J.; Cammi, R.; Pomelli, C.; Ochterski, J. W.; Martin, R. L.; Morokuma, K.; Zakrzewski, V. G.; Voth, G. A.; Salvador, P.; Dannenberg, J. J.; Dapprich, S.; Daniels, A. D.; Farkas, Ö.; Foresman, J. B.; Ortiz, J. V.; Cioslowski, J.; Fox, D. J. *Gaussian 09, Revision B.01*; Gaussian, Inc.: Wallingford, CT, 2010.
- (20) (a) Becke, A. D. *J. Chem. Phys.* **1993**, *98*, 5648. (b) Lee, C.; Yang, W.; Parr, R. G. *Phys. Rev. B* **1988**, *37*, 785.
- (21) (a) McLean, A. D.; Chandler, G. S. *J. Chem. Phys.* **1980**, *72*, 5639. (b) Krishnan, R.; Binkley, J. S.; Seeger, R.; Pople, J. A. *J. Chem. Phys.* **1980**, *72*, 650.
- (22) Kuchle, W.; Dolg, M.; Stoll, H.; Preuss, H. *J. Chem. Phys.* **1994**, *100*, 7535.
- (23) Micheli, M. C.; Marçalo, J.; Russo, N.; Gibson, J. K. *Inorg. Chem.* **2010**, *49*, 3836.
- (24) (a) Becke, A. D. *Phys. Rev. A* **1988**, *38*, 3098. (b) Perdew, J. P.; Burke, K.; Wang, Y. *Phys. Rev. B* **1996**, *54*, 16533.
- (25) (a) Jacox, M. E.; Milligan, D. E. *J. Mol. Spectrosc.* **1973**, *47*, 148. (b) Jacox, M. E. *Chem. Phys.* **1981**, *59*, 213.
- (26) Milligan, D. E.; Jacox, M. E. *J. Chem. Phys.* **1969**, *51*, 277.
- (27) (a) Milligan, D. E.; Jacox, M. E. *J. Mol. Spectrosc.* **1973**, *46*, 460. (b) Wight, C. A.; Ault, B. S.; Andrews, L. *J. Chem. Phys.* **1976**, *65*, 1244.
- (28) Hunt, R. D.; Andrews, L. *J. Chem. Phys.* **1993**, *98*, 3690.
- (29) (a) Coussan, S.; Bouteiller, Y.; Loutellier, A.; Perchard, J. P.; Racine, S.; Peremans, A.; Zheng, W. Q.; Tadjeddine, A. *Chem. Phys.* **1997**, *219*, 221. (b) Pogorelov, V.; Doroshenko, I.; Uvdal, P.; Balevicius, V.; Sablinskas, V. *Mol. Phys.* **2010**, *108*, 2165.
- (30) (a) Souter, P. F.; Kushto, G. P.; Andrews, L.; Neurock, M. *J. Am. Chem. Soc.* **1997**, *119*, 1682. (b) Raab, J.; Lindh, R. H.; Wang, X.; Andrews, L.; Gagliardi, L. *J. Phys. Chem. A* **2007**, *111*, 6383.
- (31) Liang, B.; Hunt, R. D.; Kushto, G. P.; Andrews, L.; Li, J.; Bursten, B. E. *Inorg. Chem.* **2005**, *44*, 2159.
- (32) Wang, X. F.; Andrews, L.; Marsden, C. J. *Chem.—Eur. J.* **2008**, *14*, 9192.
- (33) (a) Scott, A. P.; Radom, L. *J. Phys. Chem.* **1996**, *100*, 16502. (b) Andersson, M. P.; Uvdal, P. L. *J. Phys. Chem. A* **2005**, *109*, 2937.
- (34) Wang, G. J.; Lai, S. X.; Chen, M. H.; Zhou, M. F. *J. Phys. Chem. A* **2005**, *109*, 9514.
- (35) Wang, G. J.; Gong, Y.; Chen, M. H.; Zhou, M. F. *J. Am. Chem. Soc.* **2006**, *128*, S974.
- (36) Wang, X. F.; Andrews, L.; Li, J. *Inorg. Chem.* **2006**, *45*, 4157.
- (37) Jacox, M. E. *J. Mol. Spectrosc.* **1977**, *66*, 272.
- (38) Lloyd, J. A.; Manner, W. L.; Paffett, M. T. *Surf. Sci.* **1999**, *423*, 265.
- (39) Cotton, F. A.; Wilkinson, G.; Murillo, C. A.; Bochmann, M. *Advanced Inorganic Chemistry*, 6th ed.; Wiley: New York, 1999.
- (40) Gibson, J. K. *J. Mass Spectrom.* **1999**, *34*, 1166.
- (41) (a) Zhou, M. F.; Andrews, L.; Bauschlicher, C. W., Jr. *Chem. Rev.* **2001**, *101*, 1931. (b) Flesch, R.; Schurmann, M. C.; Hunnekuhl, M.; Meiss, H.; Plenge, J.; Ruhl, E. *Rev. Sci. Instrum.* **2000**, *71*, 1319 and references therein.